

## Wet Resist Strip Capability vs. Implant Energy

K. K. Christenson

FSI International, Chaska, Minnesota 55318, USA

Implant doses greater than  $5E14$  atoms/cm<sup>2</sup> can create an amorphous carbon like damage layer (crust) that is difficult to dissolve with wet chemistries. During the wet strip, the undamaged and lightly-damaged resist is dissolved quickly, undercutting and releasing most of the crust. The portions of crust that contact the silicon, however, cannot be undercut, and must be dissolved. The most extensive and difficult to dissolve regions of crust typically occur near the edge-bead-removal (EBR) region.

This work uses the SRIM (Stopping Range of Ions in Matter) computer simulation to investigate the characteristics of the crust for a range of implant conditions including dose, energy and implant species. Techniques to prevent the formation of attached crust near the edge bead region are also discussed.

### Introduction

It is desirable to eliminate the ash in the ash wet-clean resist strip sequence, both to eliminate a process step and to eliminate the material loss that accompanies ashing. Unfortunately, implant doses greater than  $5E14$  atoms/cm<sup>2</sup> can create an amorphous carbon like damage layer (crust) that is difficult to dissolve with wet chemistries (Figure 1). During the wet strip, undamaged and lightly-damaged resist dissolves quickly, undercutting most of the crust. Undercutting is undesirable as fragments of crust can clog filters or return to the wafers as “fall on” defects (Figure 2). The portions of crust that contact the silicon, however, cannot be undercut and must be dissolved (oval in Figure 1). The most extensive and difficult to dissolve regions of crust typically occur near the edge-bead-removal (EBR) region.

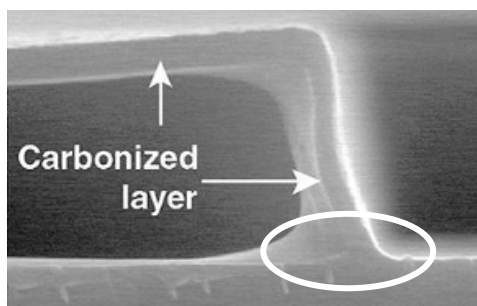


Figure 1: Damaged resist layer or “crust”.

In the course of demonstrating the strip capability of new H<sub>2</sub>SO<sub>4</sub>:H<sub>2</sub>O<sub>2</sub> (SPM) processes, we have tested resists with a wide range of implant conditions. Figure 3 shows the aggressiveness of SPM required to strip various implants. Conventional wet processes

strip implants in the lower-left portion of the plot easily. Wet stripping becomes more difficult when moving up and right in the plot, with plasma ashing being required in the plot's upper-right regions. The primary factors controlling crust formation appear to be dose, energy and implant species. Data on other factors that contribute to crust formation including the implant dose rate, beam raster speed, beam return path, wafer cooling, and resist thickness and side-wall profile, was not available for these samples. This work seeks to achieve a better understanding of the origin of the crust of damaged resist.

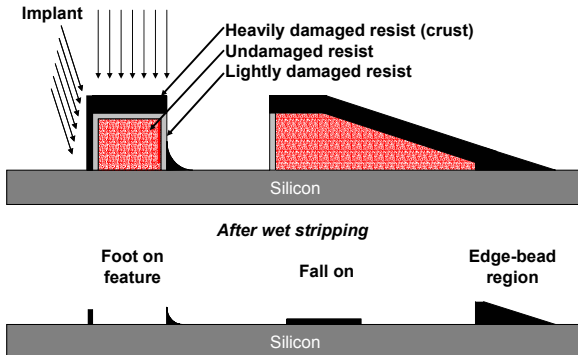


Figure 2: Ion implant damages the resist and creates an amorphous carbon crust.

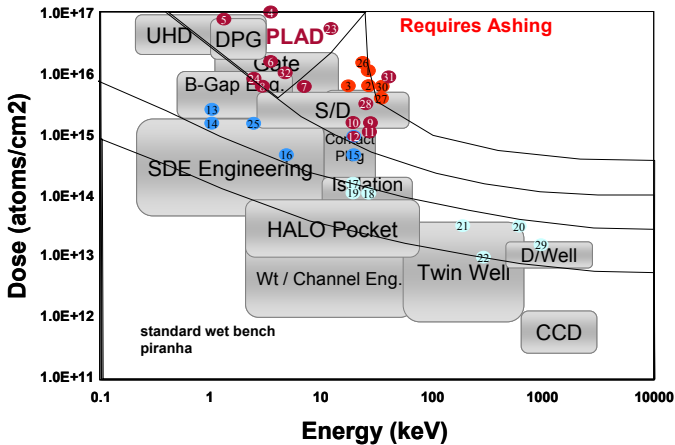


Figure 3: Strip capability of various SPM processes.

### Experimental

#### Modeling

The effects of the implanted ions on the photo resist (PR) were calculated with the SRIM (Stopping Range of Ions in Matter) computer simulation using a resist stoichiometry of  $C_5O_2H_8$ , a density of  $0.95 \text{ g/cm}^3$ , and implants of boron, phosphorus, and arsenic with energies varying from 1 to 160 keV (1, 2).

Concentration of Deposited Ions

The increase in strip difficulty with increasing dosage is easily understood as the number of damage events over 1 cm<sup>2</sup> of resist will scale linearly with the dose (the number of incident ions per cm<sup>2</sup>). The cause of the large increase in strip capability with decreasing incident energy, however, is less obvious.

Figures 4 and 5 show the depth distribution of arsenic ions implanted at 1 and 40 keV respectively. The y-axes are in units of (at/cm<sup>3</sup>)/(at/cm<sup>2</sup>). The peak concentration is found by multiplying the implant dose (at/cm<sup>2</sup>) times the value of the distribution's peak from the y axis. For the 1 keV As implant of Figure 4, a dose of 1E15 results in a peak As concentration of approximately 10<sup>21</sup> at/cm<sup>3</sup> (1E15•10x10<sup>5</sup>), or approximately 1% of the atoms in the matrix being arsenic. By comparison, the peak concentration of the 40 keV implant is approximately 2.5x10<sup>20</sup> at/cm<sup>3</sup>, only ¼ as large. Figure 6 shows the peak concentration of B, P, and As atoms in the matrix as a function of species and energy. As low energy implants are stripped more easily than high, the presence of the implanted species at the percent level is apparently not a dominant factor in the strip resistance of the crust. Further, the insoluble crust appears to extend to the surface of the feature (Figure 1), whereas the maximum concentration of implanted species occurs well into the feature.

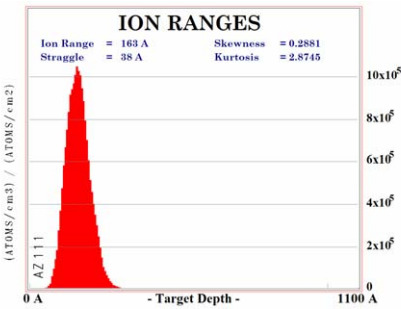


Figure 4: Depth distribution of As ions implanted at 1 keV

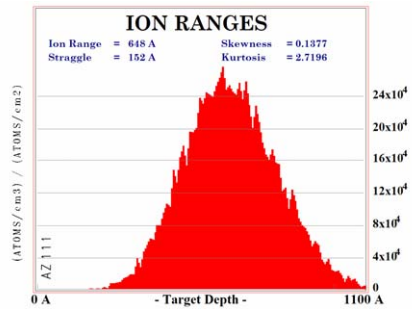


Figure 5: Depth distribution of As ions implanted at 40 keV.

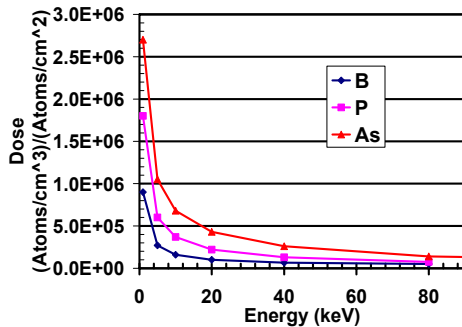


Figure 6: Peak dose as a function of energy and implanted species.

Ionization

A second damage mechanism involves the energy transferred to the electrons of the resist molecules by passing ions. SRIM refers to the energy transferred to electrons as “ionization” and the energy transferred to the nuclei as “Phonons”. Ionization can result in the breaking of chemical bonds and the loss of volatile species such as H<sub>2</sub> or O<sub>2</sub>, leaving primarily amorphous carbon. As shown in Figure 7, the ionization energy peaks near the surface of the resist, consistent with the crust shown in Figure 1. Figure 7 and Figure 8 show the ionization by As at 40 and 160 keV respectively (note difference in scale of x-axis between graphs). At high energies, the peak level of ionization varies slowly with increasing energy, whereas the width of the peak energy region increases. Consistent with Figure 3, increasing energy results in a thicker layer of crust, but does not significantly increase the peak level of damage within the crust.

Figure 9 shows the peak level of ionization energy deposited as a function of species and energy. The peak energy deposited decreases rapidly at low energies, consistent with the ability of relatively mild wet strips to remove PLAD implants.

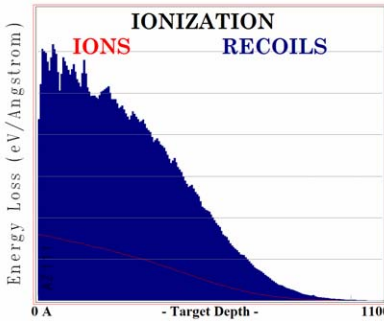


Figure 7: Ionization distribution for a 40 keV implant of As ions.

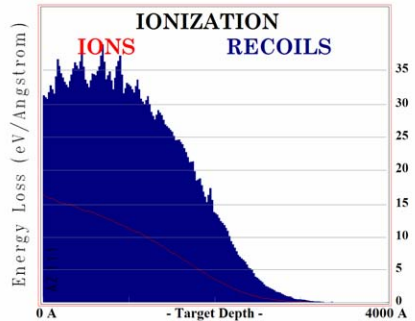


Figure 8: Ionization distribution for a 160 keV implant of As ions.

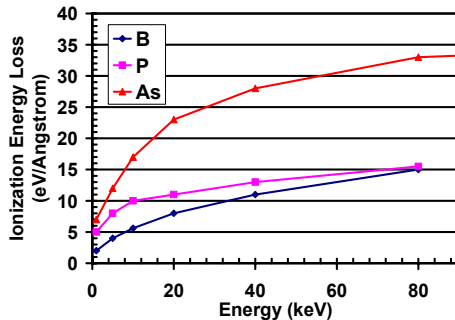


Figure 9: Peak energy loss due to ionization as a function of energy and implanted species.

Collisions

A third damage mechanism involves collisions of the implanted ions and nuclei in the resist that result in displacement of the nuclei. As with ionization, collisions can result

in the loss of H<sub>2</sub> and O<sub>2</sub> from the resist by evaporation, leaving amorphous carbon. Figure 10 thru Figure 12 show the density of collisions for implant energies of 10, 40 and 160 keV respectively (note difference in scale of x-axis between graphs). At high energies, the peak level of collision damage varies slowly with increasing energy, whereas the width of the peak damage region increases. As with ionization damage, increasing energy results in a thicker layer of crust, but does not significantly increase the peak level of damage within the crust.

Figure 13 shows the peak level of collision displacements as a function of species and energy. The peak displacement rate decreases rapidly at low energies, consistent with the ability of relatively mild wet strips to remove PLAD implants.

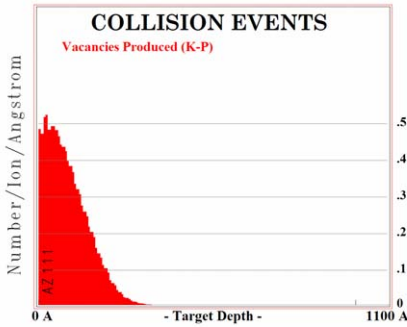


Figure 10: Collision distribution for a 10 keV implant of As ions.

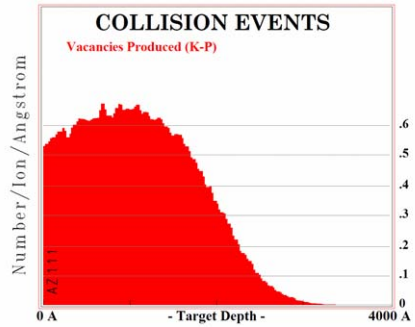


Figure 12: Collision distribution for a 160 keV implant of As ions.

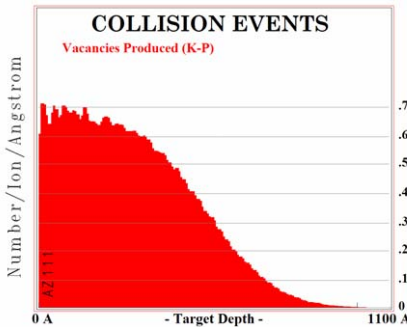


Figure 11: Collision distribution for a 40 keV implant of As ions.

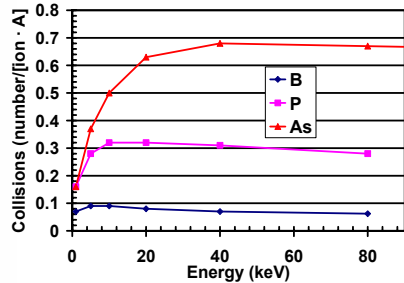


Figure 13: Collision events as a function of energy and implanted species.

### Discussion

These results indicate that the presence of the implanted species at the few atomic percent level is not a significant factor in crust formation. The variation of damage by ionization and collision displacement, however, are both consistent with the experimental data:

- The crust formation extends to the top surface of the resist
- High-dose, low energy implants can be stripped by relatively mild chemistries
- At high energies, “strip-ability” varies weakly with energy

It should be possible to determine the relative contributions of ionization and collisions by varying the implant species. As shown in Figures 9 and 13, the peak ionization damage by B and P implants are comparable, while the peak collision damage varies by more than a factor of four.

### Edge Bead Removal Region

The factors controlling the formation of the insoluble crust in the regions of the wafer containing devices are dictated by device requirements, and cannot be changed. In practice, however, the time to clear a heavily implanted wafer is often dominated by the time to clear the boundary between the resist and the edge-bead removal area (EBR). As shown in Figure 2, the shallow tapered region of the resist after EBR. This region is often 10s of microns wide, and results in a wide area of thick crust attached to the wafer. The oxidizing species in SPM attacks crust very slowly, and the time required to clear a fragment of crust is approximately proportional to the thickness of the fragment. In practice, it often requires twice the chemical exposure time to clear the thick, wide EBR region as to clear the thin feet at the base of patterned features.

It should be possible to eliminate the crust in the edge bead area through the use of a mask ring that blocks the implant from the edge bead area (Figure 14). Such rings have been used in the past on implanters to clamp the wafer, but have been abandoned as part of the effort to reduce the width of the edge exclusion region.

While it will be difficult to engineer the EBR and mask ring to prevent EBR crust formation, the cost of ownership benefits could be substantial. Even a small reduction in process time could result in an  $H_2SO_4$  savings of  $10^5$  liters/year per strip tool. Further, the elimination of this most difficult area would shift some wet strips processes from “un-manufacturable” to acceptable. This is particularly important as the industry shifts to the aggressive time budgets of single wafer processing.

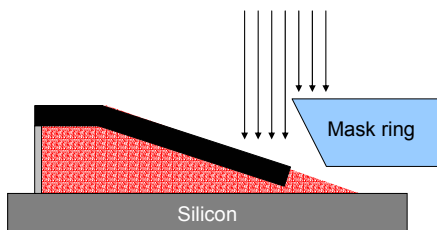


Figure 14: Mask ring to prevent the formation of attached crust near the edge of the wafer.

### **Acknowledgment**

The author would like to thank Ralph Sinclair of Implant Sciences Corporation for insightful discussions on this topic.

### **References**

1. SRIM-2006.01, J.F Ziegler, M.D Ziegler, and J.P Biersack, <http://www.srim.org>.
2. J. F. Ziegler, J. P. Biersack and U. Littmark, *The Stopping and Range of Ions in Solids*, Pergamon Press, New York (1985).